

1 **A novel D₂O tracer method to quantify RNA turnover as a biomarker of *de***
2 ***novo* ribosomal biogenesis, in vitro, in animal models, and in human skeletal muscle**

3
4 Brook MS¹, Wilkinson DJ¹, Mitchell WK¹, Lund JL¹, Phillips BE¹, Szewczyk NJ¹, Kainulainen
5 H², Lensu S², Koch LG³, Britton SL³, Greenhaff PL¹, Smith K¹, Atherton PJ¹.

6
7 ¹MRC-ARUK Centre for Musculoskeletal Ageing Research, Clinical, Metabolic and Molecular
8 Physiology, University of Nottingham, Royal Derby Hospital Centre, Derby, UK.

9 ²Biology of Physical Activity, Neuromuscular Research Centre, Faculty of Sport and Health
10 Sciences, University of Jyväskylä, Jyväskylä, Finland.

11 ³Department of Anaesthesiology, University of Michigan, Ann Arbor, Michigan, USA

12
13 **Running Title:** Quantification of ribonucleic acid synthesis in muscle

14 **Key Words :** Ribosomal biogenesis, D₂O, RNA synthesis, Muscle

15 **Word Count:** 4358

16 **Correspondence:**

17 Professor Philip J Atherton

18 MRC-ARUK Centre for Musculoskeletal Ageing Research

19 Clinical, Metabolic and Molecular Physiology

20 Royal Derby Hospital Centre

21 University of Nottingham

22 Uttoxeter Road

23 Derby, UK

24 DE22 3DT

25 **Email:** philip.atherton@nottingham.ac.uk

26

27

28

29 **Abstract**

30 Current methods to quantify in vivo RNA dynamics are limited. Here, we developed a
31 novel stable isotope (D₂O)-methodology to quantify RNA synthesis (i.e. ribosomal
32 biogenesis) in cells, animal models, and humans. Firstly, proliferating C2C12 cells were
33 incubated in D₂O-enriched media and myotubes (\pm) 50ng.ml⁻¹ IGF-1. Secondly, rat
34 quadriceps [untrained n=9; 7-wks interval-“like” training n=13] were collected after ~3-
35 wks D₂O (70-Atom%) administration, with body-water enrichment (BWE) monitored
36 via blood sampling. Finally, 10 (23 \pm 1y) men consumed 150ml D₂O followed by
37 50ml/wk and undertook 6-wks resistance-exercise (RE; 6 \times 8 repetitions, 75%-1RM
38 3/wk) with BWE monitored by saliva sampling and muscle biopsies (for determination
39 of RNA synthesis) 0-3-6-wks. Ribose mole percent excess (r-MPE) from purine
40 nucleotides was analyzed via GC-MS/MS. Proliferating C2C12 cells r-MPE exhibited a
41 rise-to-plateau while IGF-1 increased myotube RNA from 76 \pm 3ng/ul to 123 \pm 3ng/ul and
42 r-MPE by 0.39 \pm 0.1% (both P<0.01). After 3-wks, rat quadriceps r-MPE had increased
43 to 0.25 \pm 0.01% (P<0.01) and was greater with running-exercise (0.36 \pm 0.02%; P<0.01)).
44 Human muscle r-MPE increased to 0.06 \pm 0.01% and 0.13 \pm 0.02% at 3/6-wks
45 respectively equating to synthesis rates of ~0.8%/d, increasing with RE to 1.7 \pm 0.3%/d
46 (P<0.01) and 1.2 \pm 0.1%/d (P<0.05) at 3/6-wks, respectively. Therefore, we have
47 developed and physiologically validated a novel technique to explore ribosomal
48 biogenesis in a multi-modal fashion.

49

50

51

52

53 **Introduction**

54 Cellular protein content is under constant renewal to maintain cellular homeostasis.
55 Typically, the balance between protein synthesis and breakdown remains relatively
56 stable, yet under conditions of growth, atrophy or cellular proliferation, rapid and
57 significant changes in protein content and cell size occur (5). With protein synthesis
58 rates determined by the number (translational capacity) and activity (translational
59 efficiency) of ribosomes (27, 39), the ribosome provides a primary point of control in
60 cellular homeostasis; yet our understanding of dynamic ribosome metabolism is poorly
61 understood. Ribosomal biogenesis is the product of the coordinated synthesis of
62 multiple ribosomal RNA's (rRNA) and proteins. In being an energy consuming process,
63 ribosomal biogenesis is tightly regulated by multiple signaling pathways responsive to
64 nutrition, hormones and mechanical activity (22). However, basal rates of ribosomal
65 biogenesis and ribosome half-life across tissues are for the most part largely
66 undescribed. With the demands to modulate and maintain protein content varying
67 considerably across cell types, such as rapidly dividing single cells, to the coordinated
68 maintenance repair of multicellular organs, regulation of ribosome pools is likely to be
69 tightly linked with protein metabolism (10). Furthermore, when the coordinated control
70 of ribosome biogenesis becomes unregulated it can be the source of many conditions
71 such as cancer (30).

72

73 Skeletal muscle is one of the body's most plastic tissues, undergoing substantial and
74 rapid hypertrophy or atrophy under conditions of functional overload, disuse or
75 malnutrition (2, 9, 17). Understanding these processes is of great importance as
76 preservation of muscle mass and function throughout life is crucial in preventing

77 disability and maintaining quality of life- particularly in advanced ageing (16, 31). In
78 being a post-mitotic tissue, muscle mass is controlled by the balance between muscle
79 protein synthesis (MPS) and muscle protein breakdown (MPB). Many acute changes in
80 MPS (< 5h) are accompanied by the activation or suppression of proteins in the
81 mTORc1 pathway (1), modulating translational efficiency rather than translational
82 capacity (6). However, prolonged exposure to muscle loading modifies RNA content –
83 increasing with hypertrophy (3, 12, 34) and decreasing with atrophy (15). As such,
84 ribosomal biogenesis is thought to be central to muscle mass regulation.

85

86 With rRNA comprising 80% of total RNA, changes in RNA concentration are thought
87 to be indicative of changes in the balance of ribosome synthesis and breakdown.

88 However in addition to relying on long-term interventions, efficient extraction and
89 normalization to muscle weight introducing variability, measures of concentration do
90 not inform on dynamic RNA metabolism, plus changes in RNA synthesis naturally
91 precede those of content. Past measures of RNA synthesis have typically relied on the
92 incorporation of modified nucleotides such as [3H]-uridine or 5-bromouridine. However
93 the use of these techniques is limited and generally cannot be used in whole animals due
94 to their mutagenic nature. Alternatively, stable isotope tracers offer a safe method for
95 use in humans and measures of RNA synthesis using these have been made (8, 14). Yet
96 their applicability in human research has been limited due to numerous caveats,
97 including variable and complex salvage pathways, infusions and time limits (<24h)
98 resulting in a lack of methods to determine RNA synthesis rates, particularly in tissues
99 with slow renewal rates (like skeletal muscle). Heavy water (D₂O) provides alternate
100 routes in the measurement of substrate metabolism and can overcome some limitations

101 associated with other stable isotope methods. In being easily administered and with the
102 precursor pool being maintained over weeks to months, we and others have made long-
103 term cumulative measures of muscle protein synthesis (32, 40), with many other
104 substrates measured in a range of different tissues including DNA (23, 29). Deuterium
105 is incorporated via nucleotide *de novo* synthesis, overcoming previous limitations of
106 nucleotide analogues and thus similarly creates a viable route in the measurement of
107 RNA synthesis. Here, we developed sensitive GC-MS/MS universally applicable
108 methods for the measurement of RNA synthesis including in slower turning over tissues
109 requiring only minimal D₂O consumption; we validate these methods in cell cultures,
110 pre-clinical models and humans and in a cell type of contemporary interest i.e. skeletal
111 muscle.

112

113 **Materials and Methods**

114

115 **Cell culture**

116 Murine C2C12 myoblasts passage nos. 5-7; ECACC, Salisbury, UK were seeded and
117 maintained in Dulbecco's modified Eagle's medium as previously described (7)
118 containing 10% fetal bovine serum, amphotericin B (1%), penstreptomycin (1%) and
119 4mM L-glutamine (Sigma-Aldrich, UK). Sterile 70% deuterium and U-¹³C-Glucose
120 were added to DMEM at required enrichments and distributed amongst wells for
121 labeling consistency. In proliferating cells, media was changed every 48h and cells
122 scraped at required time points. At 90% confluency, cells were differentiated by
123 reducing serum concentrations to 2% with RNA synthesis stimulated 6 days after
124 differentiation with IGF1 50 ng.ml⁻¹.

125

126 **Animals**

127 Mixed population of females and males n=22 of high responder to training (HRT) rats
128 for aerobic training were used for the study. Rats originated from the generations 17 and
129 18 of selection for their training response, and were 9.2 ± 3.0 months old at the start of
130 the experiment (21). All experimental procedures described in this study protocol were
131 approved by the Animal Care and Use Committee of the Southern Finland, license
132 number ESAVI-2010-07989/Ym-23, STH 534A (21.9.2010) and complements
133 ESAVI/1968/04.10.03/2011, PH308A (30.3.2011) & ESAVI/722/04.10.07/2013,
134 PH275A (1.3.2013). All experiments were conducted in accordance with the Guidelines
135 of the European Community Council directive 86/609/EEC. Rats were kept in air-
136 conditioned rooms single-housed, at an ambient temperature of 21 ± 2 °C and the
137 relative humidity at 50 ± 10 %. Artificial lighting provided light cycles of 12 h light/12
138 h total darkness. Commercially available pelleted rodent diet (R36, Labfor/Lantmännen,
139 Malmö, Sweden) and the tap water (from the municipal water system of Jyväskylä) was
140 available *ad libitum* for rats throughout the study. The energy content of the feed was
141 1260 kJ/100 g (300.93 kcal/100g). The feed contained raw protein 18.5%, raw fat 4.0%,
142 NFE (nitrogen free extracts) 55.7%, fiber 3.5%, ash 6.3%, and water <12%. Rats
143 received a gavage of 7.2 ml/kg of 70% D₂O for the remaining 3 wks of the 7 wk
144 training period, with drinking water enriched to 2% to maintain body water enrichment.
145 Body water enrichment was determined from blood samples collected at necropsy and
146 used to represent the average enrichment throughout; although variability may occur
147 over time, enriched drinking water minimizes these effects. Interval Training consisted
148 of Warm-up for 5 min, at 50-60% of maximum speed (individually speed for each rat) +

149 running for 15 min: 3 min at 85 - 90%, 2 min pauses at 50%, repeated for 3 times;
150 inclination 15° uphill. Training was done 3 times per week, with one-day rest between
151 (if possible). 48 hrs after the last training bout animals were anaesthetized with carbon
152 dioxide and killed by cardiac puncture and thereafter immediately necropsied. Left
153 quadriceps were rapidly exposed, removed and immediately frozen by complete
154 immersion in liquid nitrogen.

155

156 **Subject characteristics and ethics**

157 Ten healthy younger (23±1y, BMI: 24±1) men were recruited as previously described
158 (3). All subjects provided their written, informed consent to participate after all
159 procedures and risks (in relation to muscle biopsies, blood sampling etc.) were
160 explained. Following inclusion to the study, subjects were studied over a 6-week period.
161 After baseline bilateral biopsies, subjects provided a saliva and blood sample then
162 consumed 150 ml D₂O (70 atom%; Sigma-Aldrich, Poole, UK) to label the body water
163 pool to ~0.2% APE which was maintained with weekly top-up boluses (50 ml.wk⁻¹).
164 Thereafter subjects performed progressive unilateral RET 3/wk at 75% 1RM, with
165 additional bilateral biopsies taken at 3 and 6 wks to monitor RNA incorporation. Blood
166 was collected at 0, 3 and 6 weeks to follow deuterium incorporation into peripheral
167 blood mononuclear cells, isolated using Histopaque (Sigma). For the temporal
168 monitoring of body water enrichment, each participant provided a saliva sample on RET
169 visits >30 min after their last meal or drink, with extra samples taken ~3 h after weekly
170 50 ml boluses to ensure that body water enrichment was accurately represented.
171 Samples were collected in sterile plastic tubes and immediately cold centrifuged at
172 16,000g to remove any debris that might be present; they were then aliquoted into 2ml

173 glass vials and frozen at -20°C until analysis. This study was approved by The
174 University of Nottingham Ethics Committee and complied with studies conducted in
175 accordance with the declaration of Helsinki and registered as clinical trials
176 (clinicaltrials.gov registration no. NCT02152839).

177

178 **Media and body water enrichment**

179 The deuterium enrichment was measured in media collected from cell culture plates and
180 plasma from rats by incubating 100µl of each sample with 2µl of 10 M NaOH and 1µl
181 of acetone for 24 h at room temperature. Following incubation the acetone was
182 extracted into 200µl of n-heptane, and 0.5µl of the heptane phase was injected into the
183 GC-MS/MS for analysis. A standard curve of known D₂O enrichment was run along
184 side the samples for calculation of enrichment. Human body water enrichment was
185 extracted by heating 100 µl saliva in an inverted 2 ml autosampler vial for 4 h at 100°C.
186 Vials were then placed upright on ice to condense extracted body water and transferred
187 to a clean autosampler vial ready for injection. A total of 0.1µl body water was injected
188 into a high-temperature conversion elemental analyzer (Thermo Finnigan; Thermo
189 Scientific, Hemel Hempstead, United Kingdom) connected to an isotope ratio mass
190 spectrometer (Delta V Advantage; Thermo Scientific)

191

192 **Protein-bound alanine muscle fraction enrichment and calculation of FSR**

193 Myofibrillar protein was isolated from human *VL* muscle biopsies and rat quadriceps by
194 homogenizing 30–50 mg muscle in ice-cold homogenization buffer, rotated for 10min,
195 and the supernatant collected after centrifugation at 13,000 g for 5 min at 4°C. The
196 myofibrillar pellet was solubilized in 0.3 M NaOH and separated from the insoluble

197 collagen by centrifugation, and the myofibrillar protein was precipitated using 1 M
198 perchloric acid (PCA). Protein-bound amino acids were released using acid hydrolysis
199 by incubating in 0.1 M HCl in Dowex H⁺ resin slurry overnight before being eluted
200 from the resin with 2 M NH₄OH and evaporated to dryness; amino acids were then
201 derivatised as their N-methoxycarbonyl methyl esters. Dried samples were suspended in
202 60 µl distilled water and 32 µl methanol, and following vortex, 10 µl pyridine and 8 µl
203 methylchloroformate were added. Samples were vortexed for 30 s and left to react at
204 room temperature for 5 min. The newly formed N- methoxycarbonylmethyl ester amino
205 acids were then extracted into 100 µl chloroform. A molecular sieve was added to each
206 sample for ~20 s before being transferred to a clean glass gas chromatography insert,
207 removing any remaining water by size exclusion absorption. Human protein-bound
208 alanine enrichment was determined by gas chromatography: pyrolysis:isotope ratio
209 mass spectrometry (Delta V Advantage Thermo Finnigan, Thermo Scientific, Hemel
210 Hempstead, UK), with rat protein-bound alanine enrichment determined by gas
211 chromatography tandem mass spectrometry (TSQ 8000 Thermo Finnigan, Thermo
212 Scientific, Hemel Hempstead, UK) alongside a standard curve of known DL-Alanine-
213 2,3,3,3-d₄ enrichment to validate measurement accuracy of the machine. Myofibrillar
214 MPS was calculated from the incorporation of deuterium-labeled alanine into protein,
215 using the enrichment of body water [corrected for the mean number of deuterium
216 moieties incorporated per alanine (3.7) and the dilution from the total number of
217 hydrogens in the derivative (i.e., 11)] as the surrogate precursor labeling between
218 subsequent biopsies. The equation used was

$$FSR = -Ln \left(\frac{1 - \left[\frac{(APE_{ala})}{(APE_p)} \right]}{t} \right)$$

219 where APE_{ala} equals deuterium enrichment of protein-bound alanine, APE_p indicates
220 mean precursor enrichment over the time period, and t is the time between biopsies.

221

222 **RNA extraction, digestion and derivatisation**

223 To extract RNA, ~20-30mg of muscle was homogenized in extraction buffer (5µl/mg)
224 containing 0.1 M Tris-HCL pH 8, 0.01 M EDTA pH 8 and 1M NaCL. Proteinase K was
225 added to a final concentration of 50 µg/µl and placed at 55°C for ~2 hrs with occasional
226 mixing until complete digestion had occurred. For cell culture, each well was scraped in
227 200 µl of extraction buffer and PBMC's homogenized in 200 µl of extraction buffer. To
228 the extractions an equal volume of phenol:chloroform:isoamyl alcohol (25:24:1) was
229 added, inverted several times to mix and the upper aqueous layer removed to a clean
230 eppendorf after centrifugation at 13000 rpm for 10 min. To remove additional protein
231 an equal volume of chloroform:isoamyl alcohol (24:1) was added to the aqueous layer
232 and repeated as above. To precipitate RNA, an equal volume of isopropanol was added
233 to the aqueous layer, inverted several times and centrifuged at 13000 rpm for 20 min.
234 The pellet was washed 3 times in 70% ethanol; air-dried, re suspended in 22 µl of
235 molecular biology and digested with 5 µl of 375 mM sodium acetate (pH 4.8), 750 µM
236 ZnSO₄ containing 0.5 units of nuclease S1 and 0.25 units potato acid phosphatase and
237 placed at 37°C overnight. Hydrolysates were then reacted with 10 µl of O-
238 benzylylhydroxylamine (2% w/v) and 7.5 µl of acetic acid at 100°C for 30 min. Samples
239 were allowed to cool at room temperature before the addition of 10µl of 1-
240 methylimidazole and 100 µl of acetic anhydride. The reactions are transferred to a
241 boiling tubed and quenched by the addition of 2 ml ddH₂O. The newly formed
242 derivatives were extracted by the addition of 750 µl dichloromethane (DCM) vortex

243 mixed and phases allowed to separate. By pre wetting the tip with DCM, the lower layer
244 is removed to a clean boiling tube and the procedure repeated. DCM extracts were then
245 dried and re suspended in 40 µl of ethyl acetate for GC-MS/MS analysis.

246

247 **GC-MS/MS instrument conditions and fractional synthesis rate calculation**

248 To measure RNA enrichment 2 µl of sample was injected into a trace 1310 gas
249 chromatograph connected to TSQ 8000 triple quadrupole GC-MS/MS (Thermo
250 Finnigan, Thermo Scientific, Hemel Hempstead, UK). Samples were injected on
251 splitless mode with inlet temperature at 280°C. GC ramp conditions were 120°C for 1
252 min, ramp to 280 °C at 10 °C /min and hold for 3 min. Selected reaction monitoring
253 (SRM) was performed for the mass to charge ratios m/z of 273.1-111.1 and 274.1-112.1
254 representing the M and M⁺¹ ions with a collision induced dissociation energy of 6.
255 Enrichment was calculated as $(M^{+1} / (M + M^{+1}))$ with the mole percent excess (MPE)
256 expressed as difference from unlabeled D₂O free samples. Fractional synthesis rates
257 were calculated as $FSR(\% \cdot d^{-1}) = (r-MPE) / [(p-MPE) \times t] \times 100$ where r-MPE is the
258 excess enrichment of bound ribose, p-MPE is the mean precursor enrichment over the
259 time period and t is the time between samples. In cell culture and rat studies, p-MPE
260 was calculated as the water enrichment multiplied by the amplification factor of 2.098
261 determined in cells. In human studies, p-MPE was taken as the ribose PBMC
262 enrichment measured over the labeling period. Samples were run in triplicate alongside
263 standard curves of known ribose standards, with the average of both peaks were used in
264 the results. Additionally, unlabeled samples were injected in different quantities to
265 determine abundance effects.

266

267 **Statistical Analysis**

268 Descriptive statistics were produced for all data sets to check for normal distribution
269 (accepted if $P > 0.05$) using a Kolmogorov-Smirnov test. All data are presented as means
270 \pm SEM. Differences between the effects of interval training and control on RNA
271 synthesis in rates were analyzed by t-test. All other data sets were analyzed by repeated
272 measures one-way or two-way ANOVA with a Bonferroni correction using GraphPad
273 Prism (La Jolla, CA) Software Version 5. Correlations were assessed using Pearsons
274 product moment correlation coefficient. The α level of significance was set at $P < 0.05$.
275

276 **Results**

277

278 **GC-MS/MS chromatography and SRM transitions**

279 Addition of O-benzylhydroxylamine and 4 acetyl groups to ribose produces a
280 derivative with a molecular weight of 423.1 (Fig 1A). Upon gas chromatography the
281 derivative produces two peaks representing the cis-trans isomers formed due to the
282 anomeric carbon of ribose (Fig 1B). Full scan MS analysis of the derivative produces a
283 most abundant fragment with best chromatography of 273.1, with second
284 fragmentation producing a most abundant fragment of 111.1. Analysis of this transition
285 is highly selective and produces GC-MS/MS spectra with very low background,
286 detecting standard enrichments as little as 0.02 APE (Fig 1C). Further this SRM
287 encompasses all backbone carbons of ribose confirmed by +5 enrichment from U-¹³C-
288 Glucose incorporation (Fig 1D).

289

290 **Deuterium incorporation into RNA bound ribose**

291 The MPE of ribose (Fig 2A) extracted from purine nucleotides of RNA from C2C12
292 cells increased linearly with increasing concentrations of media D₂O enrichment being
293 0%, 1.6±0.08%, 4.1±0.1%, 9.5±0.15%, 18.8±0.18% at media concentrations of 0%
294 0.67%, 1.9%, 4.6% and 8.9% respectively. Linear regression revealed that on average
295 2.1 ²H are incorporated into purine ribose during synthesis of new RNA. PBMC'S from
296 human subjects showed an increase in MPE to 0.37±0.04% and 0.42±0.04% (both
297 P<0.01), revealing the average accessible hydrogen's to be 2.6±0.2 (Fig 2B).

298

299 **Validation of deuterium incorporation in RNA *in vitro***

300 C2C12 cell number increased from 0.083 ± 0.001 million per well to 1.2 ± 0.03 million
301 after 117 h of proliferation (Fig 3A), whilst RNA MPE followed a rise to plateau
302 relationship from $0.28 \pm 0.03\%$ after 15 h and progressed to $0.52 \pm 0.02\%$ by 117 h (Fig
303 3B). In response to IGF1 treatment, RNA content increased by 27.5 h from 76.1 ± 3
304 $\text{ng} \cdot \text{ul}^{-1}$ to $123.4 \pm 3 \text{ ng} \cdot \text{ul}^{-1}$ (Fig 3C). Similarly, RNA MPE significantly increased in
305 control to $0.15 \pm 0.01\%$ at 27.5 h, with the increase in IGF1 treatment being significantly
306 greater (Fig 3D).

307

308 **RNA Synthesis in rat muscle *in vivo***

309 After 3 weeks of continuous D₂O administration, RNA MPE significantly increased to
310 $0.25 \pm 0.01\%$ in control and was significantly greater with interval training to
311 $0.36 \pm 0.01\%$ $P < 0.001$ (Fig 4A). The calculated RNA FSR was $0.97 \pm 0.05 \text{ \%} \cdot \text{d}^{-1}$ with a
312 significant increase in response to interval training to $1.3 \pm 0.05 \text{ \%} \cdot \text{d}^{-1}$ $P < 0.001$ (Fig 4B).
313 Rat quadriceps MPS showed a correlation with quadriceps RNA synthesis % of $r^2 = 0.17$
314 and $P = 0.05$

315

316 **RNA synthesis in human muscle**

317 The MPE from RNA bound ribose increased in rest legs to $0.064 \pm 0.01\%$ and 0.137
318 $\pm 0.02\%$ at 3 and 6 weeks respectively ($P < 0.001$). In RET legs, the MPE increased to
319 $0.125 \pm 0.02\%$ and $0.211 \pm 0.01\%$ at 3 and 6 week respectively ($P < 0.001$), being greater
320 than rest at both time points ($P < 0.005$). Corrected for PBMC RNA enrichment an FSR
321 of $0.86 \pm 0.1 \text{ \%} \cdot \text{d}^{-1}$ and $0.78 \pm 0.1 \text{ \%} \cdot \text{d}^{-1}$ was determined in rest legs at 3 and 6 weeks
322 respectively. In RET legs the RNA FSR was significantly greater than rest being 1.69

323 $\pm 0.2 \text{ \%} \cdot \text{d}^{-1}$ ($P < 0.01$) and $1.24 \pm 0.1 \text{ \%} \cdot \text{d}^{-1}$ ($P < 0.05$) at 3 and 6 weeks respectively. Human

324 VL MPS was highly correlated with VL RNA synthesis $P = 0.009$ and an $r^2 = 0.32$.

325

326

327 **Discussion**

328

329 We have developed and validated D₂O-based methods for the measurement of *in vitro*
330 and *in vivo* RNA synthesis that can be used safely and effectively in humans and with
331 the potential for application to any tissue- this is a step forward from current practices in
332 providing methods for long term measures of RNA synthesis in humans, particularly
333 those of slow turnover pools such as skeletal muscle. RNA content is closely linked to
334 cellular metabolism, with ribosomal biogenesis being required for cellular proliferation
335 (10) and growth (34). Currently, changes in RNA content are primarily determined by
336 crude measures of RNA concentrations, with limited methods in place to determine
337 dynamic rates of RNA synthesis *in vivo*. Our approach will provide insight into the
338 workings of dynamic ribosomal biogenesis *in vitro*, in animal models and in humans –
339 across cell types.

340

341 **Method development and validation of *in vitro* RNA synthesis in skeletal muscle**
342 **cells**

343 Nucleotide synthesis involves complex precursor pools with variable nucleotide salvage
344 (23) making the incorporation of stable isotope labeled compounds difficult to interpret
345 (13). The advantage of using D₂O is that deuterium becomes incorporated into the
346 backbone hydrogen of ribose during nucleotide synthesis, with deoxyribose from purine
347 deoxyribonucleosides primarily synthesized via *de novo* synthesis; as such, providing a
348 reliable input of isotope (23, 29). As deoxyribonucleotides are reduced from
349 ribonucleotides, this further creates a viable method for measures of RNA synthesis and

350 for the first time we have shown a constant incorporation of deuterium across a range of
351 media concentrations into purine ribose.

352

353 Total RNA encompasses rRNA, tRNA and mRNA that will have variable turnover rates
354 (33). The quickest of these will be tRNA and mRNA that will contribute to early
355 increases in detectable enrichment. However in making up <20% of total cellular RNA,
356 these pools become quickly saturated and deuterium incorporation follows a rise to
357 plateau in proliferating cells reflecting the required expansion of rRNA for cell division
358 (Fig 3B) (8, 10). Further, as initial validation using established stimulators of *in vitro*
359 myotube hypertrophy and ribosomal biogenesis (i.e. IGF-1)(7), we were able to detect
360 simultaneous increases in both RNA content and deuterium incorporation into RNA.
361 Therefore, deuterium incorporation into RNA was reflective of newly synthesized
362 RNA.

363

364 To use precursor product calculations, a measure of the precursor, or a proxy thereof, is
365 required (38). Alternatively, when using D₂O, an amplification factor can be used to
366 represent the amount of accessible hydrogen in the precursor that can incorporate
367 deuterium and be multiplied by the body water enrichment (4). Nucleotide precursor
368 pools are difficult to measure, with continuous input of unlabeled substrates such that
369 the maximal theoretical plateau is never achieved (24). To investigate the number of
370 accessible hydrogen in ribose *in vitro*, murine C2C12 skeletal muscle cells were
371 repeatedly passaged in a range of D₂O media enrichments, revealing a constant
372 incorporation of ~2.1 deuterium's out of a total 6. Previously, values of ~3.1 have been

373 reported for deoxyribose out of a total 7 (26, 29), expectedly higher due to the
374 additional hydrogen that exchanges with ribonucleotide reductase.

375

376 **Validation of *in vivo* RNA synthesis in an animal model**

377 Compared to many tissues, skeletal muscle has a relatively slow habitual protein
378 renewal rates, with little to no active DNA synthesis (11); in contrast actual RNA
379 synthesis rates are practically unknown and will vary considerably across tissues. As
380 D₂O can be simply administered by oral consumption and easily maintained, D₂O can
381 be used to capture a vast range of synthesis rates. Recently, D₂O has been used to
382 measure ribosome renewal in mouse liver, although in using GC-MS this requires high
383 levels of enrichment (5% APE) and fast rates of turnover (~10%) that can be
384 burdensome and limit applications(25). Applying our validated *in vitro* methods to
385 rodents, to our knowledge, we made the first long term measures of RNA synthesis in
386 skeletal muscle. In doing so, we demonstrated there is active renewal of RNA pools of
387 ~1%.d⁻¹. Furthermore, using an exercise stimulus to activate ribosomal biogenesis (39)
388 we validated the existence of a significant increase in deuterium incorporation into
389 RNA, demonstrating increased RNA synthesis. Intriguingly, RNA synthesis rates were
390 correlated with MPS, which we speculate is due to a co-ordinate regulation in response
391 to exercise.

392

393 **RNA Synthesis in Human Muscle and the Effect of Resistance Exercise**

394 Presumably most tissues will have a constant level of rRNA synthesis to maintain
395 functional ribosomes for cellular protein synthesis. That said, since ribosome biogenesis
396 consumes considerable energy and will therefore likely be maintained at minimal

397 requirements. Using the methods described here, to our knowledge we report the first
398 measures of RNA synthesis in human muscle, showing a constant synthesis rate of ~0.8
399 %. d^{-1} during “habitual activity”. Further, to assess precursor enrichment, we measured
400 the plateau enrichment of a population of cells 100% replenished (PBMCS) over the
401 labeling period (29). This accounts for individual variability in the number of accessible
402 hydrogens and further we showed on average 2.6 deuterium’s were incorporated,
403 similar to our *in vitro* measures.

404

405 Skeletal muscle RNA content is highly responsive to functional overload (28, 37) and
406 here we have shown that in response to RET, RNA synthesis was significantly
407 increased after 3 and 6 weeks of exercise training in humans. Once again, RNA
408 synthesis was correlated with MPS which further validates that in muscle, ribosome and
409 protein metabolism are likely to be inextricably related (likely via mTORc1 (18)).
410 Similarly, although there is little other data for us to compare our results to, whole body
411 rRNA turnover determined by breakdown products in urine have been estimated ~2.5%
412 (36). Further this showed a strong relationship between whole body protein degradation
413 rates of $r^2=0.7$ supporting that these are closely linked process in muscle homeostasis.

414

415 **Further Application of Methods for RNA synthesis**

416 Previously, measures of RNA synthesis have been made in humans using $6,6^2H_2$ -
417 Glucose, however this requires large amounts of tracer to be consumed (1g/Kg) and is
418 generally limited to fast turnover cells (8). Further, achieving high levels of enrichment
419 to perform GC-MS analysis in humans is costly, requiring high levels of D_2O
420 consumption that is burdensome on the individual and may potentially cause adverse

421 effects such as nausea and vertigo (19). Further, rates of RNA synthesis will vary
422 considerably across tissues, making the detection of slow turnover pools such as muscle
423 using GC-MS techniques difficult. Here, by combining sensitive GC-MS/MS
424 techniques (detection limits of $\geq 0.02\%$ MPE) and the ability to administer D₂O from
425 days to weeks, this method creates opportunities to measure RNA synthesis over a
426 range of rates and tissues. Such measures can be employed through simple D₂O
427 administration and access to tissue samples or blood- with some prior expectation of
428 synthesis helpful. For instance, human body water enrichment can be simply maintained
429 $\sim 0.15\text{-}0.2\%$ APE using an initial bolus of 150 ml D₂O, followed by weekly doses of 50
430 ml (3). In this situation, sampling from a tissue after 5 days with an RNA turnover rate
431 of $\sim 10\% \cdot \text{d}^{-1}$ would result in an easily detectable product enrichment using GC-MS/MS
432 of $\sim 0.075\text{-}0.1\%$, whereas an RNA turnover rate of $\sim 1\% \cdot \text{d}^{-1}$ would result in an
433 undetectable enrichment of $\sim 0.0075\text{-}0.01\%$. This is not to say these measure can't be
434 made by other means. Raising body water enrichment will increase end point
435 enrichment and body water enrichments as high as 2% would make GC-MS techniques
436 an option. However D₂O consumption of such high levels is costly and burdensome on
437 subjects. As such the methods used here can be readily applied to many situations.

438

439 **Conclusion**

440 In summary we have developed and validated the use of D₂O in measurement of RNA
441 synthesis both *in vitro* and *in vivo*. With many RNA synthesis rates unknown, these new
442 methods will have a significant impact in being able to measure a wide range of RNA
443 turnover rates in varied tissues. Further, ribosomal biogenesis has been the interest of
444 recent publications in muscle adaptive mechanisms (12, 20, 34, 35) and will likely play

445 a significant role elucidating muscle metabolism at rest and in response to
446 hypertrophic/atrophic conditions.
447

448 **Acknowledgments**

449 The authors are grateful for the clinical, technical and administrative support of
450 Margaret Baker, Amanda Gates and Tanya Fletcher.

451

452 **Grants**

453 This work was supported by the medical research council [grant number
454 MR/K00414X/1]; and Arthritis Research UK [grant number 19891] as part of the MRC-
455 ARUK Centre for Musculoskeletal Ageing Research; the Physiological Society
456 (awarded to P.J.A. and K.S.); the Dunhill Medical Trust [R264/1112] (to K.S., P.J.A.
457 and D.J.W.); and a Medical Research Council Confidence in Concept award
458 (CIC12019; to P.J.A., P.L.G., N.J.S. and K.S.).The founding LRT-HRT rat model
459 system was funded by the Office of Research Infrastructure Programs grant
460 P40OD021331 (to LGK and SLB) from the National Institutes of Health. Rat models
461 for low and high exercise responses (LRT/HRT) are maintained as an international
462 resource with support from the Department of Anesthesiology at the University of
463 Michigan, Ann Arbor, Michigan (see <http://koch-britton.med.umich.edu/> for
464 information). Rat tissues used in this development work were derived as part of ongoing
465 (i.e. not involving new studies) METAPREDICT studies, a European Union Seventh
466 Framework Program (HEALTH-F2-2012-277936 to H.K.).

467

468 **Disclosures**

469 No conflicting interests

470

471 **Author contributions**

472 All experiments were performed at i) the Clinical, Metabolic and Molecular Physiology
473 laboratories, Royal Derby Hospital, University of Nottingham (humans and cells), ii)
474 The Biology of Physical Activity laboratories, Neuromuscular Research Centre, Faculty
475 of Sport and Health Sciences, University of Jyvaskyla, Jyvaskyla, Finland (animal
476 experiments) and iii) the department of Anaesthesiology Laboratories, University of
477 Michigan, Ann Arbor, Michigan, USA (animal propagation). D.J.W., K.S., P.L.G.,
478 N.J.S., L.G.K., S.L.B., H.K. and P.J.A. conducted the study conception and design;
479 M.S.B., W.K.M., B.E.P., S.L. and D.J.W. performed the experiments; M.S.B., B.E.P.,
480 D.J.W., K.S. and P.J.A. analyzed the data; M.S.B., B.E.P., D.J.W., K.S. and P.J.A.
481 interpreted the results; M.S.B., B.E.P., W.K.M., D.J.W., K.S., N.J.S., J.N.L., P.L.G.,
482 H.K., S.L., L.G.K., S.L.B., and P.J.A. drafted the manuscript; M.S.B., B.E.P., W.K.M.,
483 D.J.W., K.S., N.J.S., J.N.L., P.L.G., H.K., S.L., L.G.K., S.L.B., and P.J.A. edited and
484 revised the manuscript. All authors have approved the final version of the manuscript
485 and agree to be accountable for all aspects of the work. All persons designated as
486 authors qualify for authorship, and all those who qualify for authorship are listed.
487

488 **Figure Legends**

489 **Figure 1. A)** Structure and mass of the ribose BHTA derivative. **B)** Typical GC-MS/MS
490 chromatogram of the ribose derivative on a DB-17 column for the SRM transitions of
491 (273.1-111.1). Blue line represents the M and red the M+1 **C)** Standard curve of 1-¹³C-
492 Ribose 0.02, 0.05, 0.1, 0.5 **D)** measurement of the +5 isotopomer of RNA bound ribose
493 from C2C12 myotubes incubated in U-¹³C glucose enriched media

494

495 **Figure 2. A)** MPE of RNA from maximally labeled C2C12's vs. D₂O media MPE and
496 **B)** the amplification of deuterium into PBMC'S from human subjects. *** Significantly
497 different from baseline P<0.001

498

499 **Figure 3. Time course of A)** cell number **B)** MPE of RNA in proliferating C2C12's.
500 Time course in the concentration of **C)** RNA and **D)** MPE of RNA in non-treated
501 condition (Control) and in responses to IGF1. Dotted line represents plateau
502 enrichment.* Significantly different from baseline P<0.05, *** P<0.001, ****
503 P<0.0001. § significantly different from control at that time point P<0.01

504

505 **Figure 4. A)** MPE of RNA bound ribose from control and exercised rat quadriceps **B)**
506 FSR of RNA from control and exercised rat quadriceps **C)** correlation between
507 quadriceps MPS%.d⁻¹ and RNA FSR%.d⁻¹. Dotted line represents plateau enrichment
508 *** Significantly different than control P<0.001

509

510 **Figure 5. A)** Time course of body water enrichment measured through saliva samples
511 over the 6 weeks of labeling **B)** MPE of RNA bound ribose from human VL in rest and

512 RET legs. Dotted line represents the average plateau PBMC enrichment **C)** FSR of
513 RNA bound ribose from human *VL* in rest and RET legs **D)** correlation between *VL*
514 MPS%.d⁻¹ and RNA FSR %.d⁻¹. *** Significantly different from baseline P<0.001 §
515 Significantly different from control at that time point P<0.05
516

517 **References**

- 518 1. **Atherton PJ, Etheridge T, Watt PW, Wilkinson D, Selby A, Rankin D, Smith**
519 **K, Rennie MJ.** Muscle full effect after oral protein: time-dependent concordance
520 and discordance between human muscle protein synthesis and mTORC1
521 signaling. *Am J Clin Nutr* 92: 1080–8, 2010.
- 522 2. **De Boer MD, Selby A, Atherton P, Smith K, Seynnes OR, Maganaris CN,**
523 **Maffulli N, Movin T, Narici M V, Rennie MJ.** The temporal responses of protein
524 synthesis, gene expression and cell signalling in human quadriceps muscle and
525 patellar tendon to disuse. *J Physiol* 585: 241–51, 2007.
- 526 3. **Brook MS, Wilkinson DJ, Mitchell WK, Lund JN, Szewczyk NJ, Greenhaff**
527 **PL, Smith K, Atherton PJ.** Skeletal muscle hypertrophy adaptations
528 predominate in the early stages of resistance exercise training, matching
529 deuterium oxide-derived measures of muscle protein synthesis and mechanistic
530 target of rapamycin complex 1 signaling. *FASEB J* 29: 4485–4496, 2015.
- 531 4. **Busch R, Kim Y, Neese RA, Schade-Serin V, Collins M, Awada M, Gardner**
532 **JL, Beysen C, Marino ME, Misell LM, Hellerstein MK.** Measurement of protein
533 turnover rates by heavy water labeling of nonessential amino acids. *Biochim*
534 *Biophys Acta* 1760: 730–44, 2006.
- 535 5. **Cheek DB.** Human Growth. Body Composition, Cell Growth, Energy, and
536 Intelligence. *Arch Dis Child* 45: 603–603, 1970.
- 537 6. **Chesley A, MacDougall JD, Tarnopolsky MA, Atkinson SA, Smith K.**
538 Changes in human muscle protein synthesis after resistance exercise. *J Appl*
539 *Physiol* 73: 1383–8, 1992.
- 540 7. **Crossland H, Kazi AA, Lang CH, Timmons JA, Pierre P, Wilkinson DJ,**
541 **Smith K, Szewczyk NJ, Atherton PJ.** Focal adhesion kinase is required for
542 IGF-I-mediated growth of skeletal muscle cells via a TSC2/mTOR/S6K1-
543 associated pathway. *Am J Physiol Endocrinol Metab* 305: E183–93, 2013.
- 544 8. **Defoiche J, Zhang Y, Lagneaux L, Pettengell R, Hegedus A, Willems L,**
545 **Macallan DC.** Measurement of ribosomal RNA turnover in vivo by use of
546 deuterium-labeled glucose. *Clin Chem* 55: 1824–33, 2009.
- 547 9. **DeFreitas JM, Beck TW, Stock MS, Dillon M a, Kasishke PR.** An examination
548 of the time course of training-induced skeletal muscle hypertrophy. *Eur J Appl*
549 *Physiol* 111: 2785–90, 2011.
- 550 10. **Derenzini M, Montanaro L, Chilla A, Tosti E, Vici M, Barbieri S, Govoni M,**
551 **Mazzini G, Treré D.** Key role of the achievement of an appropriate ribosomal
552 RNA complement for G1-S phase transition in H4-II-E-C3 rat hepatoma cells. *J*
553 *Cell Physiol* 202: 483–491, 2005.
- 554 11. **Drake JC, Bruns DR, Peelor FF, Biela LM, Miller R a., Miller BF, Hamilton**
555 **KL.** Long-lived Snell dwarf mice display increased proteostatic mechanisms that

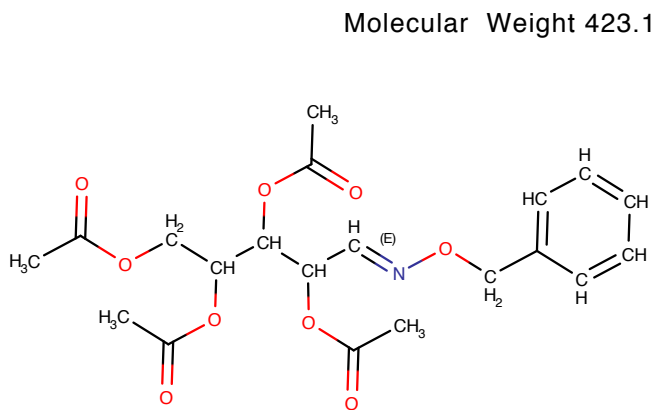
- 556 are not dependent on decreased mTORC1 activity. *Aging Cell* 14: 474–482,
557 2015.
- 558 12. **Figueiredo VC, Caldow MK, Massie V, Markworth JF, Cameron-Smith D,**
559 **Blazevich AJ.** Ribosome biogenesis adaptation in resistance training-induced
560 human skeletal muscle hypertrophy. *Am. J. Physiol. - Endocrinol. Metab.* (2015).
561 doi: 10.1152/ajpendo.00050.2015.
- 562 13. **Grimble GK, Malik SB, Boza JJ.** Methods for measuring tissue RNA turnover.
563 *Curr Opin Clin Nutr Metab Care* 3: 399–408, 2000.
- 564 14. **Grimble GK, Millward DJ.** The measurement of ribosomal ribonucleic acid
565 synthesis in rat liver and skeletal muscle in vivo [proceedings]. *Biochem Soc*
566 *Trans* 5: 913–6, 1977.
- 567 15. **Haddad F, Baldwin KM, Tesch PA.** Pretranslational markers of contractile
568 protein expression in human skeletal muscle: effect of limb unloading plus
569 resistance exercise. *J Appl Physiol* 98: 46–52, 2005.
- 570 16. **Hirani V, Blyth F, Naganathan V, Le Couteur DG, Seibel MJ, Waite LM,**
571 **Handelsman DJ, Cumming RG.** Sarcopenia Is Associated With Incident
572 Disability, Institutionalization, and Mortality in Community-Dwelling Older Men:
573 The Concord Health and Ageing in Men Project. *J Am Med Dir Assoc* 16: 607–
574 613, 2015.
- 575 17. **Houston DK, Nicklas BJ, Ding J, Harris TB, Tylavsky F a, Newman AB, Lee**
576 **JS, Sahyoun NR, Visser M, Kritchevsky SB.** Dietary protein intake is
577 associated with lean mass change in older, community-dwelling adults: the
578 Health, Aging, and Body Composition (Health ABC) Study. *Am J Clin Nutr* 87:
579 150–5, 2008.
- 580 18. **Iadevaia V, Liu R, Proud CG.** mTORC1 signaling controls multiple steps in
581 ribosome biogenesis. *Semin Cell Dev Biol* 36: 113–120, 2014.
- 582 19. **Jones PJ, Leatherdale ST.** Stable isotopes in clinical research: safety
583 reaffirmed. *Clin Sci (Lond)* 80: 277–80, 1991.
- 584 20. **Kirby TJ, Lee JD, England JH, Chaillou T, Esser K a, McCarthy JJ.** Blunted
585 hypertrophic response in aged skeletal muscle is associated with decreased
586 ribosome biogenesis. *J. Appl. Physiol.* (2015). doi:
587 10.1152/jappphysiol.00296.2015.
- 588 21. **Koch LG, Pollott GE, Britton SL.** Selectively bred rat model system for low and
589 high response to exercise training. *Physiol Genomics* 45: 606–14, 2013.
- 590 22. **Kusnadi EP, Hannan KM, Hicks RJ, Hannan RD, Pearson RB, Kang J.**
591 Regulation of rDNA transcription in response to growth factors, nutrients and
592 energy. *Gene* 556: 27–34, 2015.
- 593 23. **Macallan DC, Fullerton C a, Neese R a, Haddock K, Park SS, Hellerstein**
594 **MK.** Measurement of cell proliferation by labeling of DNA with stable isotope-

- 595 labeled glucose: studies in vitro, in animals, and in humans. *Proc Natl Acad Sci*
596 *U S A* 95: 708–13, 1998.
- 597 24. **Martini WZ, Chinkes DL, Wolfe RR.** Quantification of DNA synthesis from
598 different pathways in cultured human fibroblasts and myocytes. *Metabolism* 53:
599 128–133, 2004.
- 600 25. **Mathis AD, Naylor BC, Carson RH, Evans E, Harwell J, Knecht J, Hexem E,**
601 **Peelor FF, Miller BF, Hamilton KL, Transtrum MK, Bikman BT, Price JC.**
602 Mechanisms of *In Vivo* Ribosome Maintenance Change in Response to Nutrient
603 Signals. *Mol Cell Proteomics* 16: 243–254, 2017.
- 604 26. **Messmer BT, Messmer D, Allen SL, Kolitz JE, Kudalkar P, Cesar D, Murphy**
605 **EJ, Koduru P, Ferrarini M, Zupo S, Cutrona G, Damle RN, Wasil T, Rai KR,**
606 **Hellerstein MK, Chiorazzi N.** In vivo measurements document the dynamic
607 cellular kinetics of chronic lymphocytic leukemia B cells. *J Clin Invest* 115: 755–
608 764, 2005.
- 609 27. **Millward DJ, Garlick PJ, James WPT, Nnanyelugo DO, Ryatt JS.**
610 Relationship between protein synthesis and RNA content in skeletal muscle.
611 *Nature* 241: 204–205, 1973.
- 612 28. **Nakada S, Ogasawara R, Kawada S, Maekawa T, Ishii N.** Correlation between
613 Ribosome Biogenesis and the Magnitude of Hypertrophy in Overloaded Skeletal
614 Muscle. *PLoS One* 11: e0147284, 2016.
- 615 29. **Neese R a, Misell LM, Turner S, Chu a, Kim J, Cesar D, Hoh R, Antelo F,**
616 **Strawford a, McCune JM, Christiansen M, Hellerstein MK.** Measurement in
617 vivo of proliferation rates of slow turnover cells by 2H2O labeling of the
618 deoxyribose moiety of DNA. *Proc Natl Acad Sci U S A* 99: 15345–50, 2002.
- 619 30. **Orsolic I, Jurada D, Pullen N, Oren M, Eliopoulos AG, Volarevic S.** The
620 relationship between the nucleolus and cancer: Current evidence and emerging
621 paradigms. *Semin Cancer Biol* 37-38: 36–50, 2016.
- 622 31. **Rizzoli R, Reginster J-Y, Arnal J-F, Bautmans I, Beudart C, Bischoff-**
623 **Ferrari H, Biver E, Boonen S, Brandi M-L, Chines A, Cooper C, Epstein S,**
624 **Fielding R a, Goodpaster B, Kanis J a, Kaufman J-M, Laslop A, Malafarina**
625 **V, Mañas LR, Mitlak BH, Oreffo RO, Petermans J, Reid K, Rolland Y, Sayer**
626 **AA, Tsouderos Y, Visser M, Bruyère O.** Quality of life in sarcopenia and frailty.
627 *Calcif Tissue Int* 93: 101–20, 2013.
- 628 32. **Robinson MM, Turner SM, Hellerstein MK, Hamilton KL, Miller BF.** Long-
629 term synthesis rates of skeletal muscle DNA and protein are higher during
630 aerobic training in older humans than in sedentary young subjects but are not
631 altered by protein supplementation. *FASEB J* 25: 3240–9, 2011.
- 632 33. **Ross J.** mRNA stability in mammalian cells. *Microbiol Rev* 59: 423–50, 1995.
- 633 34. **Stec MJ, Kelly N a, Many GM, Windham ST, Tuggle SC, Bamman MM.**
634 Ribosome biogenesis may augment resistance training-induced myofiber

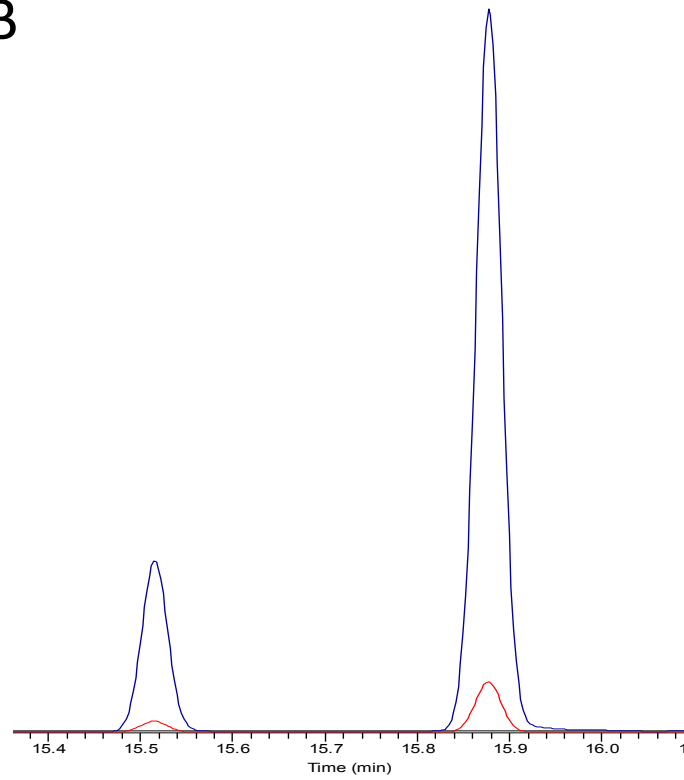
- 635 hypertrophy and is required for myotube growth in vitro. *Am. J. Physiol. -*
636 *Endocrinol. Metab.* (2016). doi: 10.1152/ajpendo.00486.2015.
- 637 35. **Stec MJ, Mayhew DL, Bamman MM.** The effects of age and resistance loading
638 on skeletal muscle ribosome biogenesis. *J Appl Physiol* 59: jap.00489.2015,
639 2015.
- 640 36. **Topp H, Fusch G, Schöch G, Fusch C.** Noninvasive markers of oxidative DNA
641 stress, RNA degradation and protein degradation are differentially correlated
642 with resting metabolic rate and energy intake in children and adolescents.
643 *Pediatr Res* 64: 246–250, 2008.
- 644 37. **Von Walden F, Casagrande V, Ostlund Farrants a.-K, Nader G a.** Mechanical
645 loading induces the expression of a Pol I regulon at the onset of skeletal muscle
646 hypertrophy. *AJP Cell Physiol* 302: C1523–C1530, 2012.
- 647 38. **Watt PW, Lindsay Y, Scrimgeour CM, Chien P a, Gibson JN, Taylor DJ,**
648 **Rennie MJ.** Isolation of aminoacyl-tRNA and its labeling with stable-isotope
649 tracers: Use in studies of human tissue protein synthesis. *Proc Natl Acad Sci U*
650 *S A* 88: 5892–6, 1991.
- 651 39. **West DWD, Baehr LM, Marcotte GR, Chason CM, Tolento L, Gomes A V.,**
652 **Bodine SC, Baar K.** Acute resistance exercise activates rapamycin-sensitive
653 and insensitive mechanisms that control translational activity and capacity in
654 skeletal muscle. *J Physiol* 00: n/a–n/a, 2015.
- 655 40. **Wilkinson DJ, Franchi M V, Brook MS, Narici M V, Williams JP, Mitchell**
656 **WK, Szewczyk NJ, Greenhaff PL, Atherton PJ, Smith K.** A validation of the
657 application of D₂O stable isotope tracer techniques for monitoring day-to-day
658 changes in muscle protein subfraction synthesis in humans. *Am J Physiol*
659 *Endocrinol Metab* 306: E571–9, 2014.
- 660
- 661
- 662
- 663
- 664
- 665
- 666
- 667
- 668

Figure 1

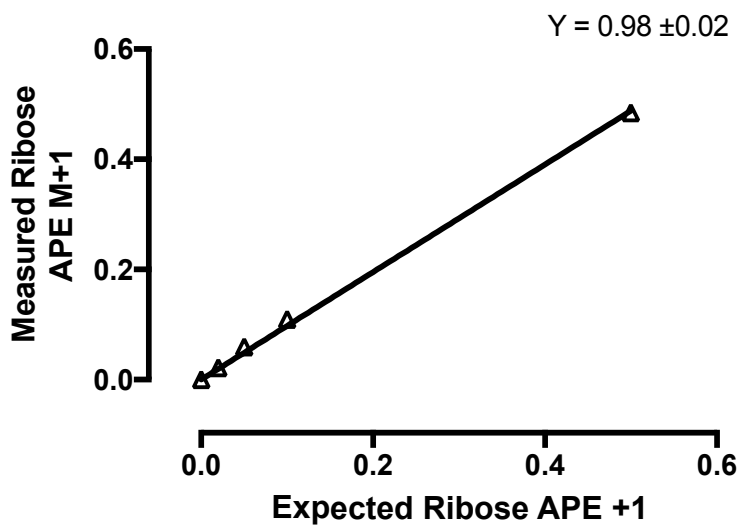
A



B



C



D

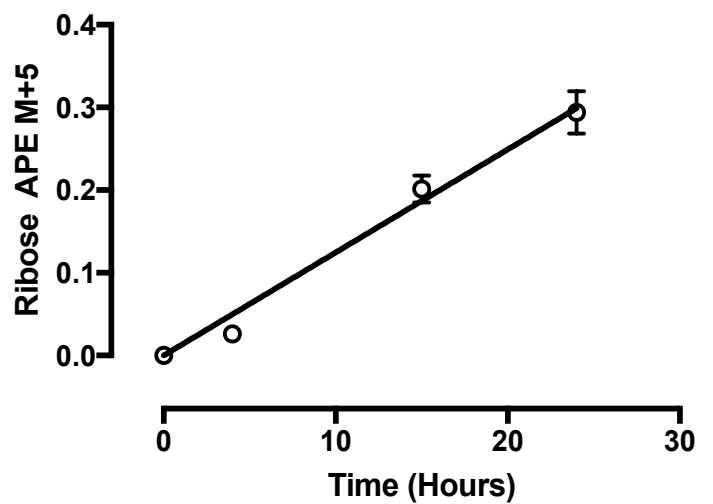


Figure 2

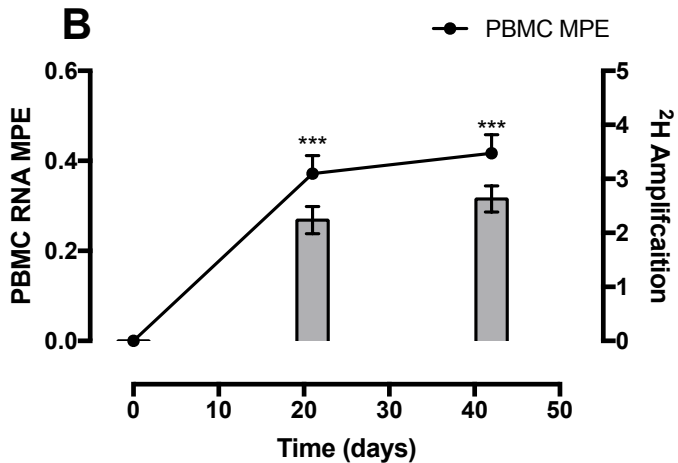
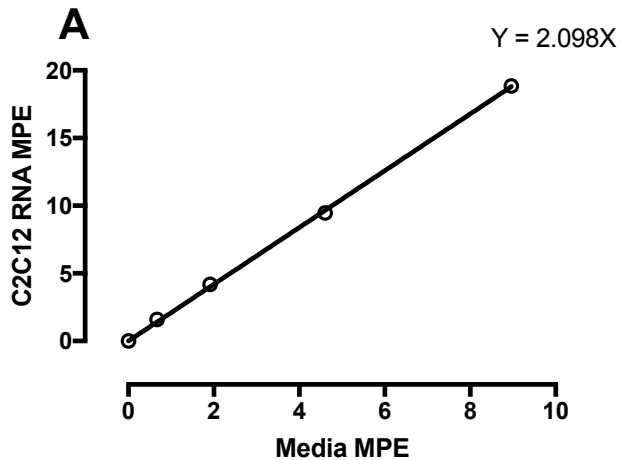
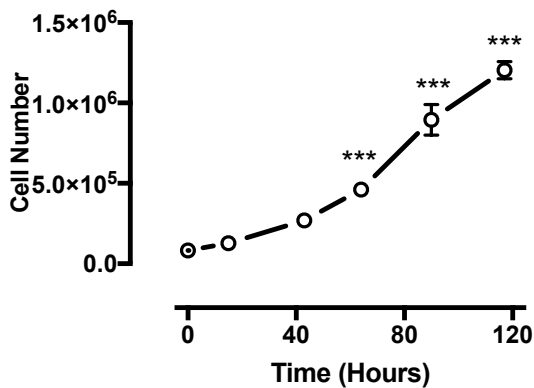
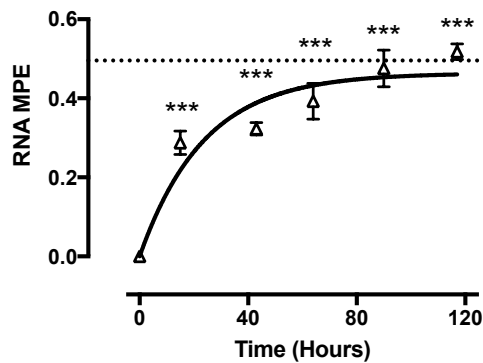


Figure 3

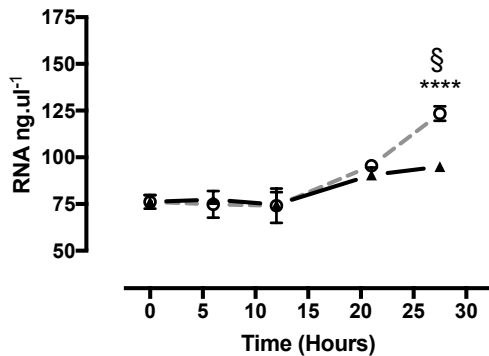
A



B



C



D

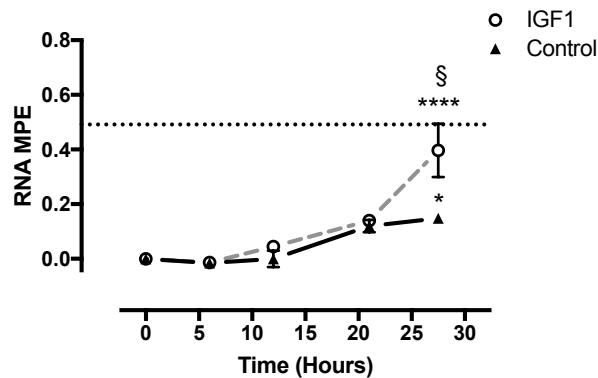


Figure 4

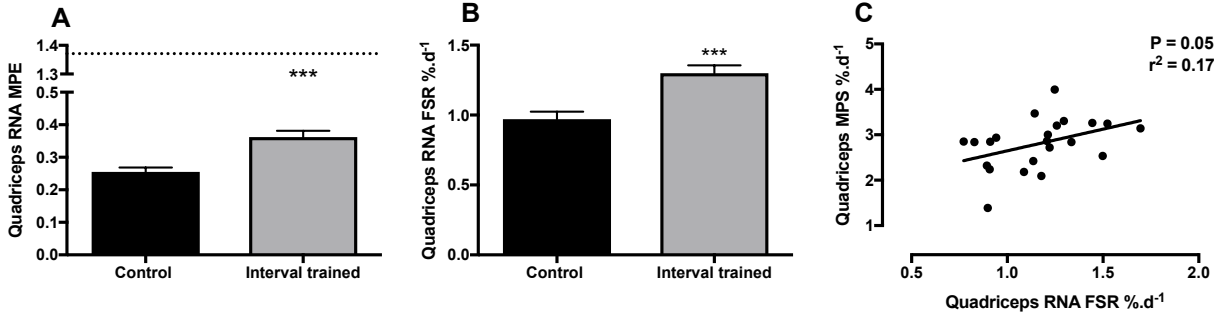


Figure 5

